IEEE *Access*

Multidisciplinary ┊ Rapid Review ┊ Open Access Journal

Parametric Estimation from Empirical Data Using Particle Swarm Optimization Method for Different Magnetorheological Damper Models (April 2021)

Asan G.A. Muthalif[1], M. Khusyaie M. Razali [2], N. H. Diyana Nordin[3], Syamsul B.A. Hamid[4]

[1]Department of Mechanical and Industrial Engineering, College of Engineering, Qatar University, Doha, Qatar

[2,3,4] Smart Structures, Systems and Control Research Lab (S[3]CRL), Department of Mechatronics Engineering, Kulliyyah of Engineering, International Islamic University Malaysia, Kuala Lumpur, Malaysia

Corresponding author: Asan G. A. Muthalif (e-mail: drasan@qu.edu.qa).

ABSTRACT The nonlinearity behaviour of magnetorheological fluid (MRF) can be described using a number of established models such as Bingham and Modified Bouc-Wen models. Since these models require the identification of model parameters, there is a need to estimate the parameters' value carefully. In this paper, an optimization algorithm, i.e., the Particle Swarm Optimization (PSO) algorithm, is utilized to identify the models' parameters. The PSO algorithm distinctively controls the best fit value by minimizing marginal error through root-mean-square error between the models and the empirical response. The validation of the algorithm is attained by comparing the resulting modified Bouc-Wen model behaviour using PSO against the same model's behaviour, identified using Genetic Algorithm (GA). The validation results indicate that the application of PSO is better in identifying the model parameters. Results from this estimation can be used to design a controller for various applications such as prosthetic limbs.

INDEX TERMS magnetorheological fluid damper, parametric estimation, particle Swarm Optimization, Genetic Algorithm

I. INTRODUCTION

Magnetorheological fluids (MRFs) are smart materials utilized to implement semi-active systems to enable their controllability [1]. MRFs have gained massive interests during the last decades and been incorporated in many applications, including dampers, control valves, brakes and clutches [2-5]. MRFs are considered highly controllable as their fluid state can be changed to be semi-solid when subjected to magnetic fields [6]. For this reason, MRFs have been incorporated in the implementation of semi-active dampers for vehicle suspensions. Magnetorheological (MR) dampers are semi-active control devices that are widely used in various applications such as transtibial prosthetic limb [7-8], tremor attenuation [9], seismic structural control [10], automotive suspension application [11] and landing gear [12]. Filled with MR fluid, MR dampers have gained interest due to their controllability, response time, low power consumption and fault-safe characteristics [13]. However, the applications of MR damper are restricted by its nonlinear hysteresis force-velocity and force-displacement characteristic. Thus, to fully utilize the advantages of MR fluid, an accurate mathematical

model that is able to represent the device fully is required. To date, various models have been researched and proposed to represent the hysteretic characteristic of MR damper. Among them, parametric modelling has been widely used to describe the damper's characteristic due to its model accuracy, effectiveness, and less complexity than other non-parametric models [13].

Due to the growing interests in MR dampers, various investigations have been conducted to explore their hysteretic behavior to improve the control accuracy and consider the parameter variations in the system to enhance the control robustness. Choi *et al* [14] developed an MR damper with a hysteresis model to predict the field-dependent damping force. Song *et al* [15] proposed an adaptive control algorithm for an MR damper system that considers both hysteresis and the system's varying parameters. Yu *et al* [16] established an MR damper with a model-free fuzzy control algorithm and evaluated the MR suspension system's effective performance by road testing. Shen *et al* [17] investigated the characteristics of a load-levelling suspension system with an MR damper system in which the stiffness and damping can be adjusted by

controlling the MR damper. Hong *et al* [18] experimentally investigated an MR damper's effectiveness through a nondimensional Bingham model. Choi *et al* [19] presented a controllable MR damper considering both the field-dependent hysteretic behavior and the suspension system's parameter variation.

Highly nonlinear hysteresis of MRF damper behavior is one of the challenging aspects that need to be encountered to model their characteristics. In most cases, metaheuristic optimization methods are widely employed in parametric identification of highly nonlinear hysteretic of MRF damper [20]. The optimization is calculated by minimizing the error between the model outputs and the experimental data. Among the most preferred algorithm is the Genetic Algorithm (GA) [21-23]. State estimation (SE) is also considered as a robust estimation method when multiple conforming gross errors exist, or multiple leverage points exist. Chen *et al* [24] proposed a robust SE method based on second-order conic programming that ensures an optimal global solution and has high estimation accuracy. A robust state estimator was also proposed based on maximum exponential absolute value [25] and other based on weighted least absolute values that have good robustness and high efficiency [26]. In the application of MR fluid, bio-inspired computing optimizing algorithm has gained interest as it is a promising approach that can be further developed for new and robust competing techniques. Apart from the Genetic Algorithm, other bio-inspired algorithms, including Grasshopper optimization algorithm [27], shuffled Frog Leaping Algorithm [28], and Crow Search Algorithm [29] have shown potential in describing the MR damper used. However, these algorithms are complicated.

On the other hand, Particle Swarm Optimization (PSO) offers less complexity and yields a similar accuracy level [30-31]. The PSO optimization has been implemented in various applications, including design optimization of tuned mass damper [32], and cable-damper systems [33]. Modified PSO was proposed by Pathak *et al* [34] which generates new swarm positions and fitness solutions using improved and modified search equations. In this step, the swarm searches in the proximity of the best solution of the previous iteration to improve the exploitation behaviour. The particle swarm employs greedy selection procedure to choose the best candidate solution [35]. A constriction factor-based particle swarm optimization (CFPSO) algorithm was proposed by Pathak *et al* [36]. The addition of the constriction factor helps in accelerating the convergence property of CFPSO. Based on the literature survey conducted, the methodology for parametric estimation of the MRF damper model is still ongoing. Thus, this research discusses the implementation of PSO for parametric estimation to be implemented in the MRF damper model. ACO, PSO and GA are categorized as Metaheuristic methods that do not rely on the type of the problem. Such search algorithms are used for complex problems (often involve many variables for optimization) that are not well suited for standard algorithms.

In this work, a number of established models were investigated. They are Bingham, Simple Bouc-Wen, Modified Bouc-Wen, Nonlinear Biviscous and Hyperbolic Tangent Function. The modified Bouc-Wen model was used to present the damper. These models' parameters were then estimated using Particle Swarm Optimization and compared with that of the Genetic Algorithm to determine which technique is more efficient. The strategy was to achieve a simulated behavior that is approximate to the empirical data. This was realized by minimizing the normalized root-mean-squared error.

In this paper, Section 2 describes the methodology. Section 3 compares the parametric estimation algorithms' performance: Particle Swarm Optimization (PSO) and Genetic Algorithm (GA). This section also compares the performance of the MR damper models. The parametric equations of the best-suited model are presented. The paper ends with conclusions from the findings and states possible future work thereof.

II. METHODOLOGY

A. PARTICLE SWARM OPTIMIZATION

Particle Swarm Optimization (PSO) was first introduced by Eberhart and James Kennedy [37]. PSO is classified as stochastic properties, where the initial value of estimation is random rather than manually guessing. Also, it reduces the probability of estimating at a local optimum and offers ease of utilization, less computation time, high accuracy, and quick convergence [30, 38-39].

The algorithm of PSO is shown in Fig.1. PSO randomly generates the position of a particle (parameter) (x_i (t)) into a group of number of population (swarm) within a given bound. The next position of the particle (x_i (t+1)) is estimated according to its inertia as well as both local and global memories, as in Eq. (1) and (2).

$$x_i(t + 1) = x_i(t) + v_i(t + 1) \qquad (1)$$

$$
\begin{aligned}
v_i(t + 1) = &\ w v_i(t) \\
&+ r_1 c_1 \big(p_{best}(t) - x_i(t)\big) \\
&+ r_2 c_2 \big(g_{best}(t) - x_i(t)\big)
\end{aligned} \qquad (2)
$$

Here, v_i (t+1) describes the velocity of the particle's position in both direction and speed. The velocity term consists of Inertia, Cognitive and Social Components.

The first term of Eq. (2) is the Inertia Component, which controls the momentum of the particle's velocity ($v_i(t)$) and w is the inertial weight factor [40]. The second part is the Cognitive Component, which controls the effect of personal experience or the local best position (p_{best}) (the best position for every i^{th} iteration). Also, the best position in the population is the one with the minimum cost value. The third component, which is the Social Component, controls the global best position (g_{best}) i.e., the overall best position of the particle. The value of g_{best} is constantly substituted with p_{best}

whenever the current cost value of g_{best} is lower than the previous one [41]. The design parameters, r_1 and r_2 are random numbers, ranging from 0 to 1. On the other hand, the design parameters c_1 and c_2 are the acceleration constants, which can be expressed as in Eq. (6) and (7) [42]. The parameters are compiled in Table I below.
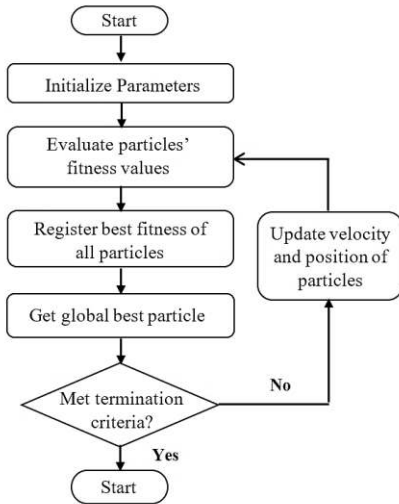

FIGURE 1. The flowchart of the PSO algorithm.

According to Clerc and Kennedy [43], the inertial weight factor, w is equal to the constriction coefficients (ω):

$$\omega = \frac{2k}{12 - \emptyset - \sqrt{\emptyset^2 - 4\emptyset}} \tag{3}$$

where,

$$0 \le k \le 1 \tag{4}$$
$$\emptyset = \emptyset_1 + \emptyset_2 \ge 4 \tag{5}$$

In this work, k is equal to 1, and the values of $\emptyset_1$ and $\emptyset_2$ are set to 2.05. The parameters of c_1 and c_2 are as follows:

$$c_1 = \omega\emptyset_1 \tag{6}$$
$$c_2 = \omega\emptyset_2 \tag{7}$$

The particle's position is continuously updated until the targeted objective function is achieved. In this paper, the objective function is to minimize the normalized root-mean-squared error.

TABLE I
PSO PARAMETERS

Properties	Value
r_1 and r_2	Design random parameters ranging from 0 to 1
c_1 and c_2	Acceleration constants
$\emptyset_1$ and $\emptyset_2$	Random positive numbers set to 2.05
ω	Inertial weight factor

The objective function or performance criteria should first be defined as it directly affects the evolutionary change in optimization operation. The commonly used objective functions are the root-mean-square error (RMSE), which describes the error between the empirical and simulation result. The equation is given by:

$$RMSE = \sqrt{\frac{1}{N}\sum_{i=1}^{N}[EFR_i(t) - SFR_i(t)]^2} \tag{8}$$

where $i \ (i = 1 - N)$ is the number of experimental samples, $EFR_i(t)$ is the empirical result – Empirical Force Response at the ith sampling spot and $SFR_i(t)$ is the simulation result – Simulated Force Response. For a fair comparison, NRMSE or normalized error is given in Eq. 9 is applied, where EFR_{max} is the maximum empirical value.

$$NRMSE = \frac{RMSE}{EFR_{max}} \tag{9}$$

B. EXPERIMENTAL SETUP

In this work, LORD RD-8040-1 [44] is used. This damper is a short-stroke damper with a maximum length of 55 mm. The picture of the damper is shown in Fig. 2. RD-8040-1 damper can withstand high tensile strength up to approximately 8896 N. Table II, and III describe the properties of the damper.

FIGURE 2. The picture of MR damper RD-8040-1.

TABLE II
TYPICAL PROPERTIES OF MR DAMPER (RD-8040-1) (LORD CORPORATION 2009).

Properties	Value
Stroke, mm (in)	55 (2.17)
Extended Length, mm (in)	208 (8.2)
Body Diameter, mm (in)	42.1(1.66) max
Shaft Diameter, mm (in)	10 (0.39)
Tensile Strength, N (lbf)	8896 (2000) max
Damper Forces, N (lbf)	
• 5 cm/sec @ 1 A	>2447 (>550)
• 20 cm/sec @ 0A	<667 (<150)
Operating Temperature, °C	71 (160) max

- @ 71 °C (160 °F)

The MRF damper is subjected to harmonic excitation on Fatigue Testing Machine (FTM) to obtain empirical results, as shown in Fig. 3. The test machine used in the experiment is 'Shimadzu Servopulser' and controlled by Servopulser Control unit, '4830 Controller'. The Control Computer is used to record the data from the control unit and
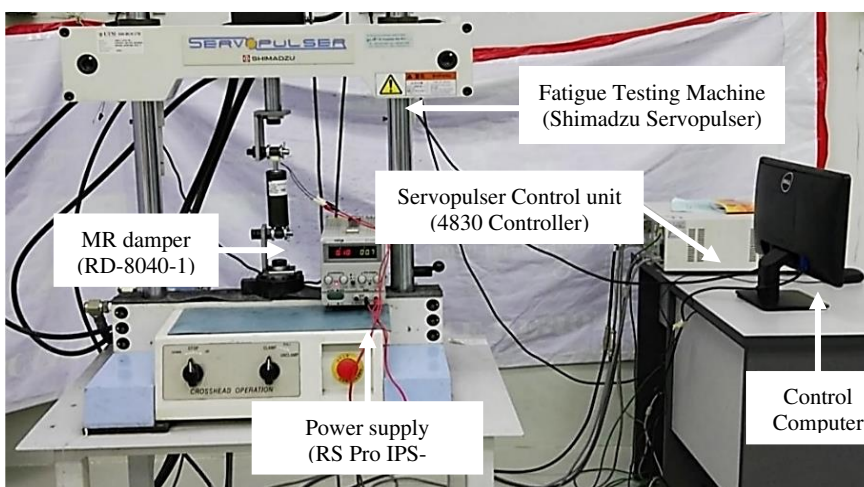
TABLE III
ELECTRICAL PROPERTIES OF MR DAMPER (RD-8040-1) (LORD CORPORATION 2009).

Properties	Value
Input Current (A)	
• Continuous for 30 seconds	1 max
• Intermittent	2max
Input Voltage (V)	12 DC
Resistance (Ω)	5
• @ ambient temperature	7

FIGURE 3. The experimental setup of the MR damper.

use them to plot force versus time, force versus displacement and force versus velocity graphs. An 'RS Pro IPS-303DD' power supply is used to feed current to the MRF damper. The damper is attached to the upper and lower ends of the machine via fabricated damper's grippers. The damper's piston rod is excited sinusoidally, while a load cell and a linear variable differential transformer (LVDT) sensor integrated into the machine measure the force and displacement of the piston rod, respectively. 'Windows Software for 4830' running on the Control Computer records the force, displacement and relative velocity of the piston rod.

Tests are done to acquire the damper's dynamic response by changing the applied current from 0 to 1 A in increments of 0.1 A, while maintaining the frequency at constant levels of 0.4 until 2 Hz in increments of 0.4 Hz. The experiment is repeated by varying the excitation from 0.4 to 2 Hz in increments of 0.4 Hz while keeping the current at a constant value of 0 to 1 A in increments of 0.1 A. The tested stroke range is 50 mm at a constant starting position in the middle of the stroke. The tests are performed by providing a harmonic displacement input excitation,

$$u = A_m sin(2\pi ft) \qquad (10)$$

where A_m is the excitation amplitude of the displacement, and f is the frequency of the excitation. Thus, the velocity of the damper is written as:

$$v = 2\pi f A_m cos(2\pi ft) \qquad (11)$$

TABLE IV
INPUT VARIABLES OF THE TEST.

Variables	Value
Current (A)	0.0, 0.1, 0.2, 0.3, 0.4, 0.5, 0.6, 0.7, 0.8, 0.9, 1.0
Frequency (Hz)	0.4, 0.8, 1.2, 1.6, 2.0

III. RESULTS AND DISCUSSION

The results of the experiment are shown in Fig. 4 and Fig. 5. Here, the patterns show that the force response increases uniformly as the current increases at a constant frequency. When the current is constant, the force response increases with increasing frequency. Thus, it shows that the damper's force response depends on the current and the excitation frequency. Also, higher velocity leads to a higher force response.

In order to estimate the parameters of the dynamic models of the MR damper, the strategy is to make the simulated behavior of the system as close as possible to the empirical data. This can be realized by minimizing the normalized root-mean-squared error (NRMSE). Both Genetic Algorithms (GA) and Particle Swarm Optimization (PSO) are used in the parameter identification process to determine which technique works better. The modified Bouc-Wen model is used to represent the damper.

The PSO tuning for parameter estimation is based on the PSO constant obtained in section 2. On the other hand, the GA algorithm utilized is directly taken from the MATLAB Toolbox. Total iteration for each run for both algorithms is set at 100, with the population's size at 100. A similar range of parameters is set when running both algorithms.

Comparisons between the empirical data, with its corresponding parametric model response (using both PSO and GA), are presented in Fig. 6. It is observed that the predicted response using PSO agrees well with the empirical values compared with GA. The resulting normalized errors are shown in Table V. Based on the results, it is concluded that PSO is better than GA in solving this problem.
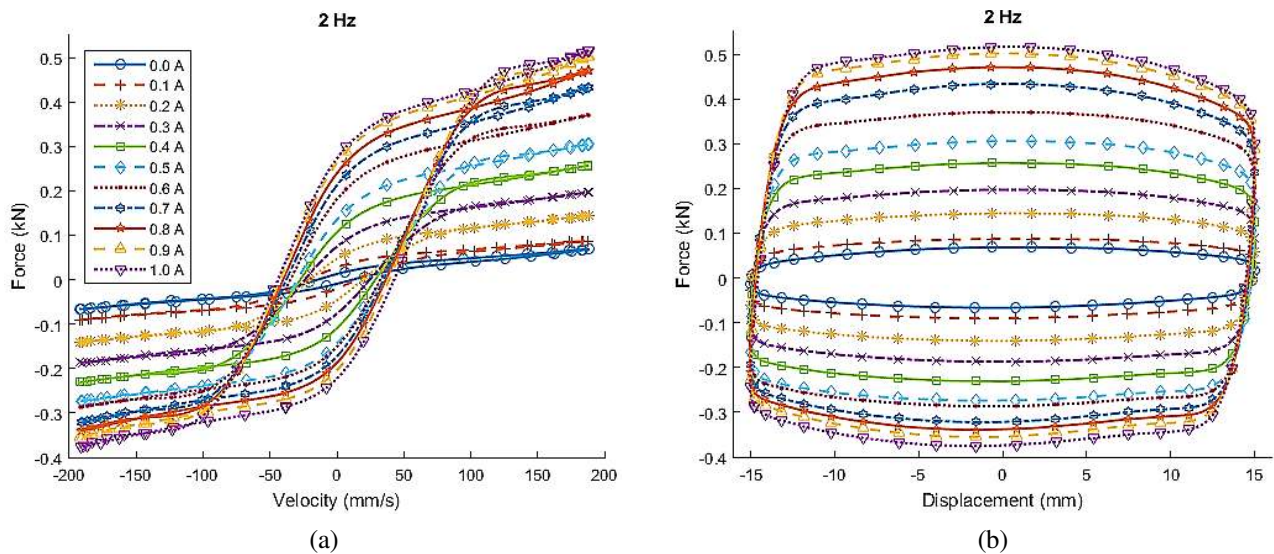

FIGURE 4. Hysteresis loop of the force response of RD-8040-1 with respect to (a) velocity and (b) displacement at 2 Hz with varied current.
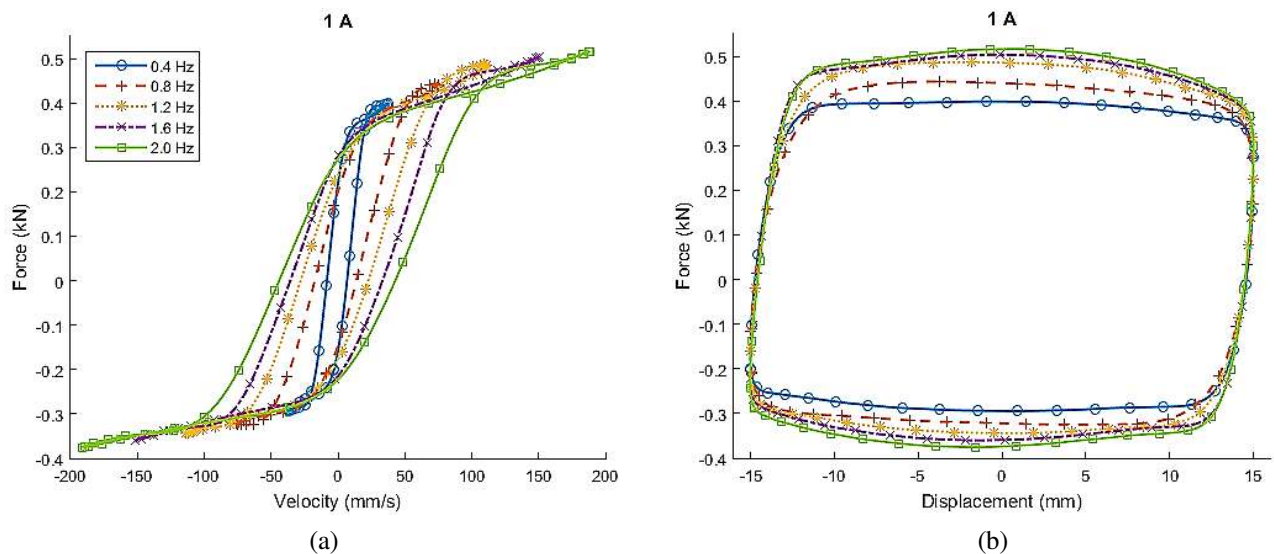

FIGURE 5. Hysteresis loop of the force response of RD-8040-1 with respect to (a) velocity and (b) displacement at 1 A with varied frequency.

The performance of the MR damper models is evaluated by comparing the model output with the empirical data. The plots of the investigated MR damper models, at which its associated parameters are estimated using PSO, are shown in Fig. 7. The estimation error for all models is presented in Table VI. Generally, in Fig. 7, all models' results are in good

agreement with the empirical data. However, based on the error comparison in Table VI, the Modified Bouc-Wen model seems to be the best in representing the MR damper.

TABLE V
NORMALIZED-RMSE BETWEEN PSO AND GA. NOTE: ERROR = [PSO, GA]

	2 Hz		1 A
0.0 A	[0.0214, 0.0327]	0.4 Hz	[0.0245, 0.0329]
0.2 A	[0.0157, 0.0317]	0.8 Hz	[0.0262, 0.0354]
0.4 A	[0.0253, 0.0420]	1.2 Hz	[0.0343, 0.0538]
0.6 A	[0.0323, 0.0391]	1.6 Hz	[0.0377, 0.0508]
0.8 A	[0.0372, 0.0438]	2.0 Hz	[0.0408, 0.0529]

TABLE VI
NORMALIZED-RMSE BETWEEN ALL MODELS.

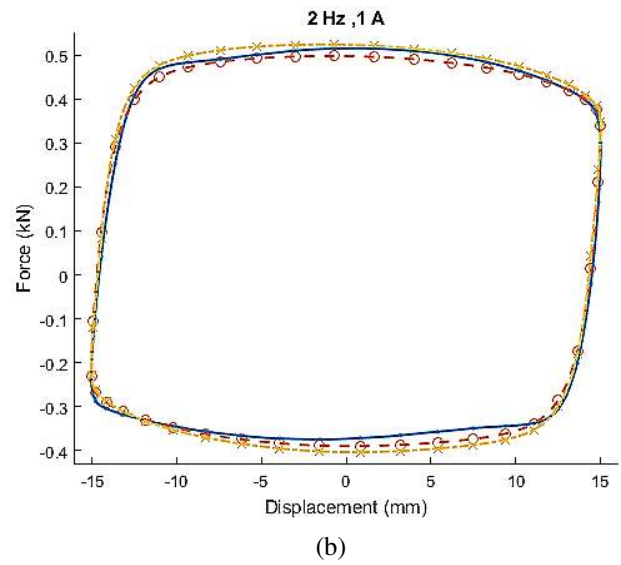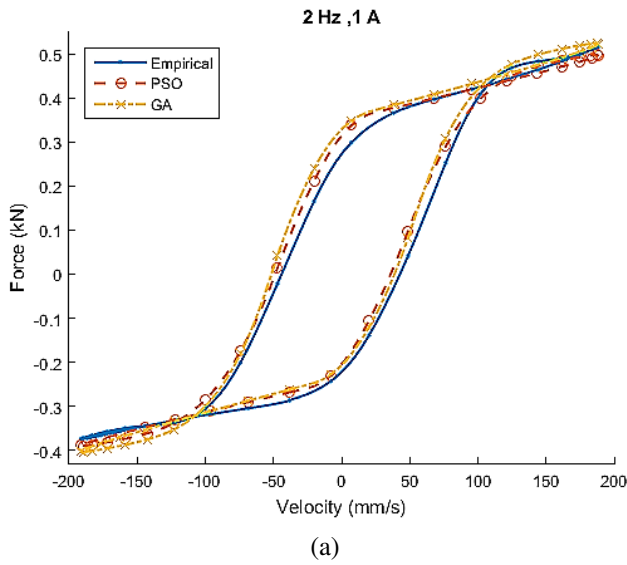| MR damper Model	Error (2 Hz, 0.5 A)	Error (2 Hz, 1 A)
Bingham	0.1881	0.2045
Simple Bouc-Wen	0.0456	0.0454
Modified Bouc-Wen	0.0306	0.0408
Nonlinear Biviscous	0.2120	0.2335
Hyperbolic Tangent Function	0.1010	0.0971

(a)

(b)

FIGURE 6. Comparison graph between PSO and GA of the force response of RD-8040-1 with respect to (a) velocity and (b) displacement at 2 Hz and 1A.
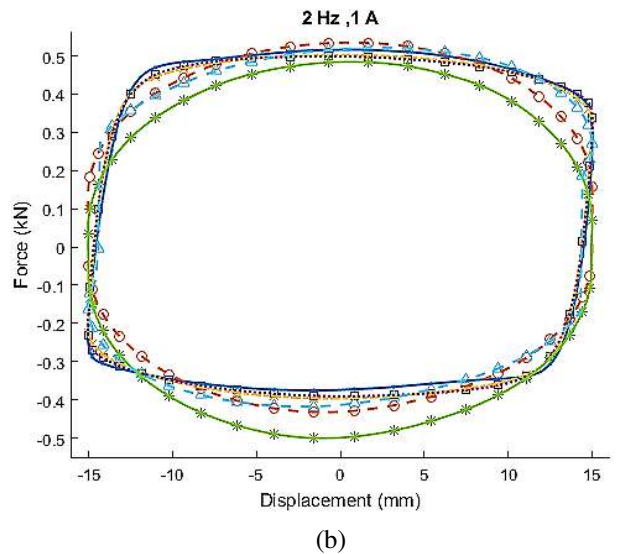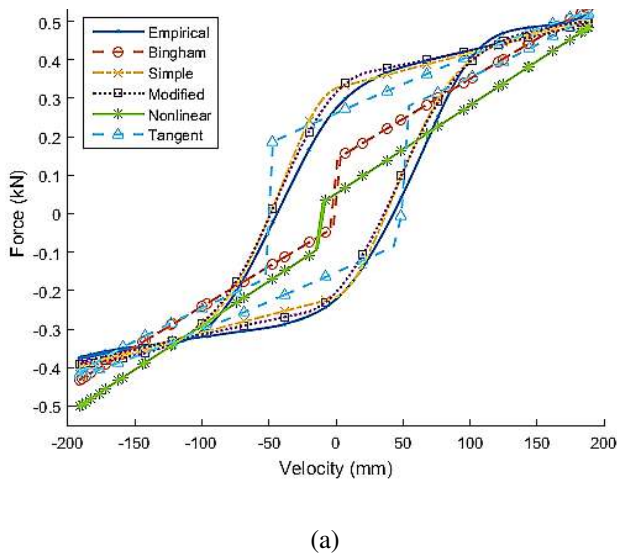

(a)

(b)

FIGURE 7. Comparison graph of the force response between the MR damper models and the empirical data with respect to (a) velocity and (b) displacement at 2 Hz and 1 A.

A. MODIFIED BOUC-WEN MODEL AS THE BEST MODEL TO DESCRIBE MR DAMPER

The Modified Bouc-Wen model can be written as:

$$F = c_1 y + k_1(x - x_o) \tag{12}$$

$$\dot{y} = \frac{1}{c_1 + c_o}(\alpha z + c_o \dot{x} + k_o(x - y)) \tag{13}$$

$$\dot{z} = -\gamma |\dot{x} - \dot{y}||z|^{n-1}z - \beta(\dot{x} - \dot{y})|z|^n \\ + A(\dot{x} - \dot{y}) \tag{14}$$

where force response is represented by F, internal and external displacement is represented by y and x, respectively, and initial displacement of the piston is donated by x_o. Damping coefficients at low and large velocity are represented by c_1 and c_2. Spring stiffness is represented by k_1 and k_o, where k_1 is related to the nominal damper force because of the accumulator, while k_o is to control the stiffness at high velocity. Also, coefficient z is the hysteresis deformation of the damper where the smoothness of the hysteresis is controlled by coefficient γ, β, A and n [45].

However, it is found out that the response of the Modified Bouc-Wen model does not compensate for the accumulator effect in the region where the magnitude of the current or frequency is high. For better prediction, a modified version of the model is proposed as

$$F = c_1 y + k_1(x - x_o) + f_o \tag{15}$$

where an offset force (f_o) is added to overcome the accumulator effect (Note that offset force is already added in the Modified Bouc-Wen model during parametric identification in Section 2). Fig. 8 shows the plot of the Modified Bouc-Wen model's force response with and without parameter fo. At different current and frequency, the corresponding model with and without parameter f_o is compared (see Table VII). The result shows the model with offset force has a better prediction than the model without offset force.
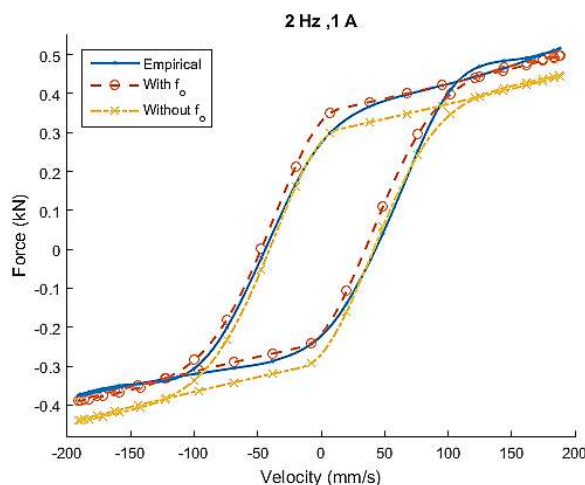
FIGURE 8. Comparison graph of the force response between Modified Bouc-Wen model with and without parameter f_o.

TABLE VII
COMPARISON OF NORMALIZED- RMSE BETWEEN MODIFIED BOUC-WEN MODEL WITH AND WITHOUT PARAMETER f_o. NOTE: ERROR = [WITH f_o, WITHOUT f_o].

2 Hz			1 A	
0.0 A	[0.0214, 0.0377]		0.4 Hz	[0.0245, 0.0711]
0.2 A	[0.0157, 0.0210]		0.8 Hz	[0.0262, 0.0625]
0.4 A	[0.0253, 0.0433]		1.2 Hz	[0.0343, 0.1131]
0.6 A	[0.0323, 0.0965]		1.6 Hz	[0.0377, 0.0662]
0.8 A	[0.0372, 0.1158]		2.0 Hz	[0.0408, 0.1061]

In this section, the optimal polynomial order is discussed. As mentioned before, the Modified Bouc-Wen model is found out the best to represent the MR damper. The model's force response highly depends on two main variables: magnetic field (electrical current) and velocity of the piston (frequency). Thus, the parameters of the model from Eqs. (13) to (15) are assumed as a function of current and frequency directly.

The relation for each parameter is described in the form of polynomial equations. However, the polynomial order needs to be investigated to avoid the complexity of the models without jeopardizing their precision. So, a simple test is done by curve fitting the parameters, from first to fifth polynomial order. The test result is shown in terms of computation time and error, as in Fig. 9.

The curve fitting error represents the accuracy of the estimated equation at the different polynomial order, while]e the force response error represents the accuracy of the estimated force response using the estimated equation. The result shows higher polynomial order returns lower curve fitting error and lower force response error. However, higher polynomial order results in longer computation time as well as a complex parametric equation. Thus, based on the breakeven point in Fig. 9, the maximum polynomial order is set at third order. At this point, the computation time is considerably fast with a low force response error.
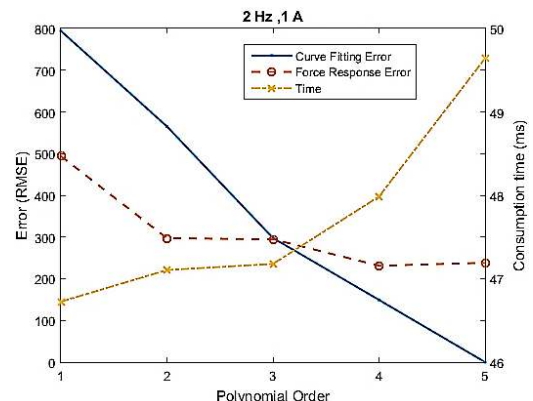
FIGURE 9. The curve fitting error and the force response error of the Modified Bouc-Wen model for different polynomial order with the computation time.

The proposed equations for Modified Bouc-Wen parameters are as follow:

$$\beta = 4849 - 7181i - 6711f + 12710i^2 \\ -3351if + 6999f^2 - 6816i^3 \\ +1304i^2f + 567if^2 - 1987f^3 \tag{16}$$

$$\gamma = 1935 - 5041i - 1416f + 5105i^2 \\ + 3102if + 691.4f^2 - 2027i^3 \\ -833.1i^2f - 941.6if^2 \tag{17}$$

$$A = 4571 + 12170i - 13450f - 9567i^2 \\ + 1860if + 13230f^2 + 3103i^3 \\ -1018i^2f + 1010if^2 - 3651f^3 \tag{18}$$

$$k_1 = -763.1 + 7391i - 2259f - 9788i^2 \\ -1964if + 3227f^2 + 2903i^3 \\ +4754i^2f - 280.1if^2 - 999.6f^3 \tag{19}$$

$$k_o = 2382 - 11770i - 1424f + 15660i^2 \\ -1224if + 276.4f^2 - 5140i^3 \\ -7164i^2f + 2444if^2 \tag{20}$$

$$c_o = 175 + 279.8i + 65.43f + 2142i^2 \tag{21}$$

$$-152.4if - 844i^3 - 390.1i^2f$$

$$c_1 = 24850 + 33860i - 65570f \\ +21510i^2 - 41610if + 55930f^2 \\ -21170i^3 + 7301i^2f + 13040if^2 \\ -14610f^3 \tag{22}$$

$$f_o = 4.989 - 124.6i - 2.643f + 325.2i^2 \\ +33.53if - 179.4i^3 - 16.38i^2f \tag{23}$$

where f is the frequency, and i is the input current. Parameter α, x_o, and n are constants which are 80, 0 and 1 respectively.

The error between the empirical force response and the predicted force response is computed as a function of time. The resultant errors are shown in Table VIII. Overall, it is observed that the model response is practically acceptable compared to the empirical data even though it contains some discrepancies. This discrepancy is believed due to the fitting errors of the Modified Bouc-Wen model. The investigation shows that the average normalized error for the optimization to portray the MRF damper's behaviour is approximately less than 0.05 or more than 95% optimization accuracy. It can be implied that the optimization is leaning at its finest representation on modelling the MRF damper. Fig. 10 shows the result of the force response using the proposed equation. While Fig. 11 shows the curve fitting graph of the Modified Bouc-Wen model parameters.

TABLE VIII
THE NORMALIZED-RMSE AND THE ACCURACY OF THE PREDICTED MODEL (MODIFIED BOUC-WEN MODEL).

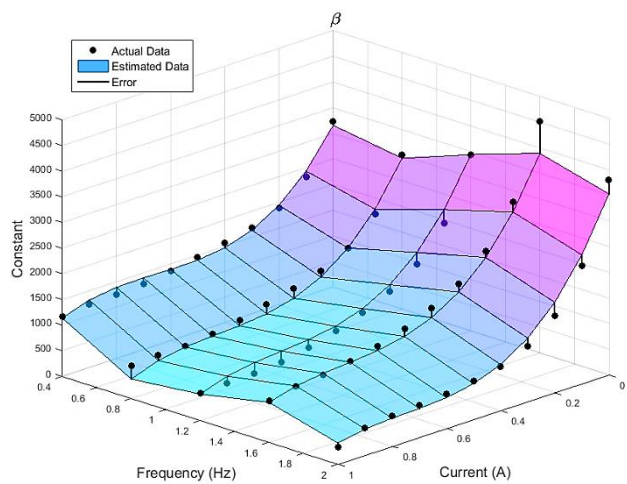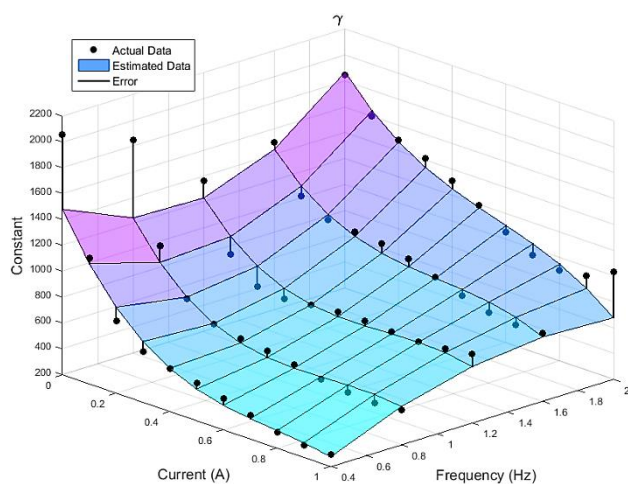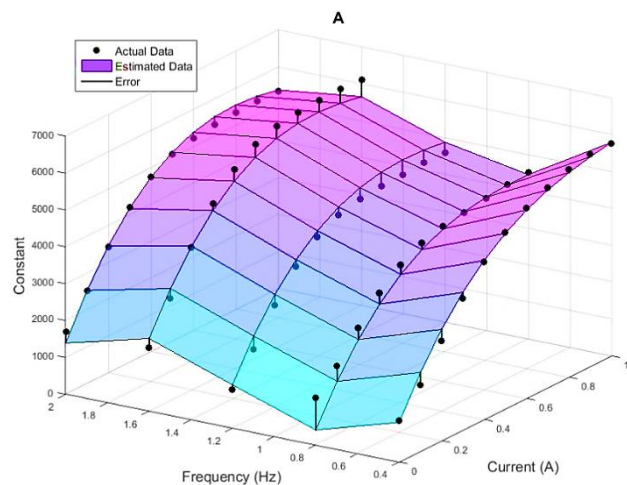| Frequency (Hz)	Current (A)										
	0.0	0.1	0.2	0.3	0.4	0.5	0.6	0.7	0.8	0.9	1.0
	Normalized-RMSE (N/N)										
0.4	0.129	0.070	0.043	0.025	0.021	0.020	0.020	0.019	0.028	0.017	0.024
0.8	0.097	0.044	0.024	0.023	0.021	0.021	0.021	0.021	0.024	0.020	0.026
1.2	0.059	0.027	0.023	0.025	0.023	0.028	0.025	0.029	0.032	0.034	0.033
1.6	0.032	0.025	0.015	0.024	0.020	0.023	0.026	0.028	0.028	0.032	0.034
2.0	0.021	0.021	0.015	0.019	0.025	0.036	0.032	0.034	0.037	0.038	0.041
	Optimization Accuracy (%)										
0.4	87.01	92.97	95.65	97.41	97.83	97.95	97.93	98.01	97.20	98.20	98.18
0.8	90.23	95.52	97.55	97.64	97.89	97.81	97.87	97.88	97.56	97.99	97.97
1.2	94.00	97.21	97.62	97.41	97.64	97.12	97.43	97.05	96.73	96.51	96.69
1.6	96.75	97.44	98.47	97.57	97.90	97.63	97.32	97.15	97.11	96.77	97.06
2.0	97.84	97.88	98.03	98.09	97.44	96.33	96.77	96.50	96.29	96.11	95.86
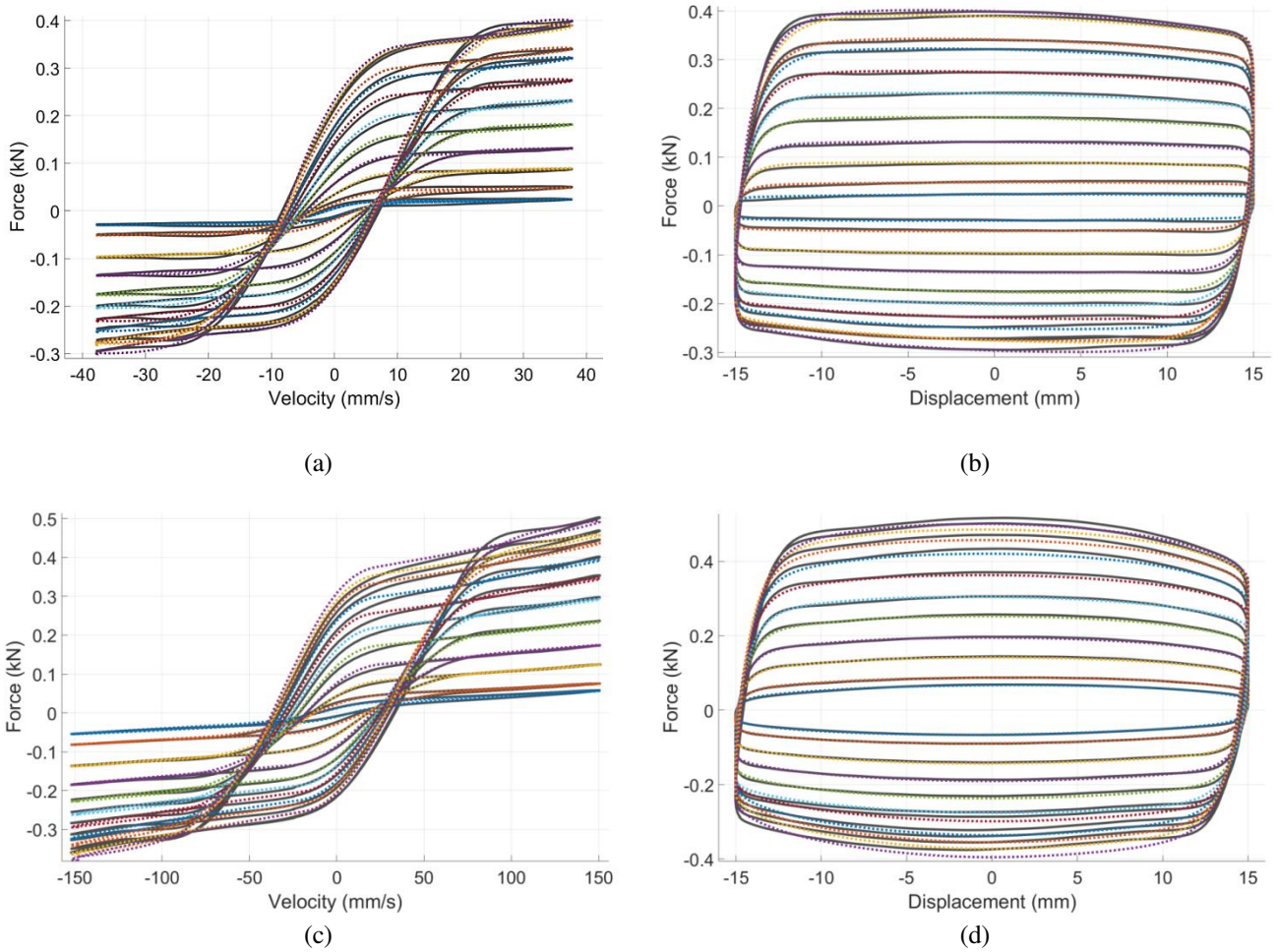
FIGURE 10. Hysteresis loop of the force response of the Modified Bouc-Wen model for (a) velocity and (b) displacement at 0.4 Hz, and (c) velocity and (d) displacement at 2 Hz with the varied current.
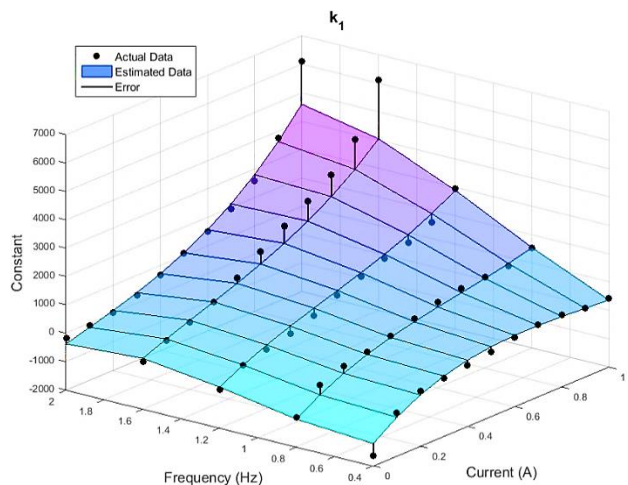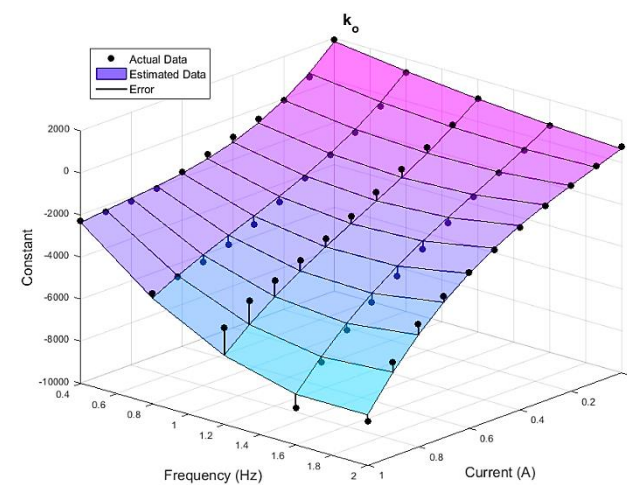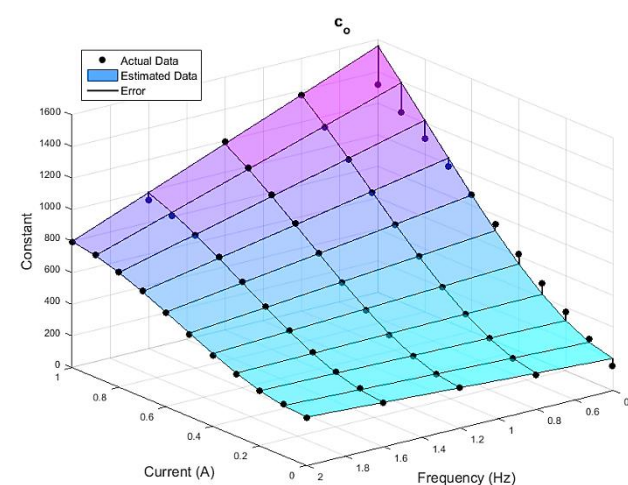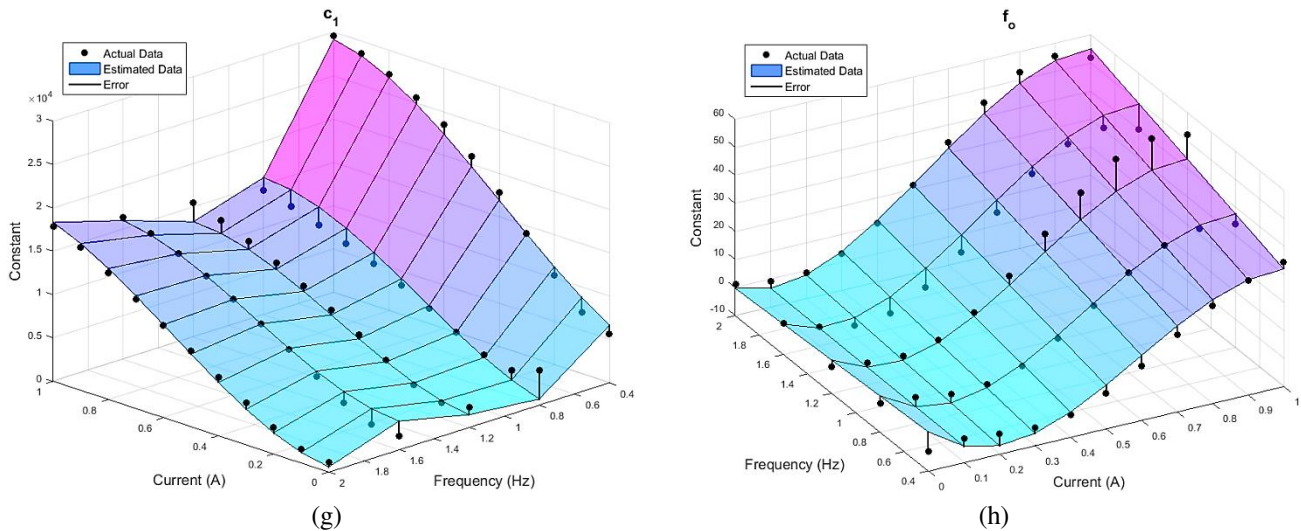
(a)

(b)

(c)

(d)

(e)

(f)

FIGURE 11. Parametric value of Modified Bouc-Wen model as function of current and frequency; (a) β, (b) γ, (c) A, (d) k_1, (e) k_o, (f) c_o, (g), c_1 (h) f_o.

IV. CONCLUSION

This paper discusses the implementation of Particle Swarm Optimization (PSO) and Genetic Algorithm (GA) in estimating the parameters of magnetorheological fluid damper models. In this article, PSO was used to estimate parameters used to describe the behaviour of the MRF damper based on a modified bouc-wen model. The PSO performances in the estimation are shown and compared with GA; a detailed analysis of the estimation w.r.t current and frequency are illustrated in the article. Both PSO and GA algorithms show good agreement with the experimental results. However, PSO has lower relative errors compared to GA. Comparing the MR dampers' mathematical models shows that the Modified-Bouc Wen model can precisely predict the MR damper's behavior. Equations representing the dynamic of the MR damper are presented using a third-order polynomial curve fitting from experimental results. For future work, the analytical model given in this article can be used for simulation study and controller design in applications involving shock absorption. Results from this estimation can be used to design a controller for various applications such as prosthetic limbs.

ACKNOWLEDGEMENT

REFERENCES

[1] J. Yang *et al.*, "A semi-active suspension using a magnetorheological damper with nonlinear negative-stiffness component," *Mech. Syst.* *Signal Process.*, vol. 147, p. 107071, Jan. 2021. DOI: 10.1016/j.ymssp.2020.107071.

[2] M. Ashtiani, S. H. Hashemabadi, and A. Ghaffari, "A review on the magnetorheological fluid preparation and stabilization," *J. Magn. Magn. Mater.*, vol. 374, pp. 711–715, Jan. 2015. DOI: 10.1016/j.jmmm.2014.09.020.

[3] H. Lv *et al.*, "The Dynamic Models, Control Strategies and Applications for Magnetorheological Damping Systems: A Systematic Review," *J. Vib. Eng. Technol.,* vol. 9, no. 1, pp. 131–147, Jan. 2021. DOI: https://doi.org/10.1007/s42417-020-00215-4.

[4] W. W. Chooi and S. O. Oyadiji, "Design, modelling and testing of magnetorheological (MR) dampers using analytical flow solutions," *Comput. Struct.*, vol. 86, no. 3–5, pp. 473–482, Feb. 2008. DOI: 10.1016/j.compstruc.2007.02.002.

[5] I. Bica, Y. D. Liu, and H. J. Choi, "Physical characteristics of magnetorheological suspensions and their applications," Ind. Eng. Chem. Res., vol. 19, no. 2, pp. 394-406, Mar. 2013. DOI: 10.1016/j.jiec.2012.10.008.

[6] J. Sathya Kumar *et al.*, "A review of challenges and solutions in the preparation and use of magnetorheological fluids," *Int. J. Mech. Mater. Eng.*, vol. 14, no. 1, p. 13, Nov. 2019. DOI: 10.1186/s40712-019-0109-2.

[7] Q. Fu, D. H. Wang, L. Xu, and G. Yuan, "A magnetorheological damper-based prosthetic knee (MRPK) and sliding mode tracking control method for an MRPK-based lower limb prosthesis," *Smart Mater. Struct.*, vol. 26, no. 4, p. 045030, Mar. 2017. DOI: 10.1088/1361-665X/aa61f1.

[8] N. D. Nordin, A. G. Muthalif, and M. K. M Razali, "Control of transtibial prosthetic limb with magnetorheological fluid damper by using a fuzzy PID controller," *J. Low Freq. Noise, Vib. Act. Control*, vol. 37, no. 4, pp. 1067–1078, Dec. 2018. DOI: 10.1177/1461348418766171.

[9] A. Yi *et al.*, "A novel exoskeleton system based on magnetorheological fluid for tremor suppression of wrist joints," in *IEEE Int Conf Rehabil Robot,* Toronto, ON, Canada, 2019, pp. 1115-1120.

[10] C. Daniel *et al.*, "Magnetorheological fluid with nano Fe3O4 for performance enhancement of MR damper for seismic resistance of steel structures," *Key Eng. Mater.*, vol. 763, pp. 975–982, Feb. 2018. DOI: 10.4028/www.scientific.net/KEM.763.975.

[11] J. C. Tudon-Martinez *et al.*, "Magneto-rheological dampers - Model influence on the semi-active suspension performance," *Smart Mater. Struct.*, vol. 28, no. 10, p. 105030, Sep. 2019. DOI: 10.1088/1361-665X/ab39f2.

[12] Y. T. Choi *et al.*, "Analysis and control of a magnetorheological landing gear system for a helicopter," *J. Am. Helicopter Soc.*, vol. 61, no. 3, Jul. 2016. DOI: 10.4050/JAHS.61.032006.

[13] G. Wang, G. Chen, and F. Bai, "Modeling and identification of asymmetric Bouc-Wen hysteresis for piezoelectric actuator via a novel differential evolution algorithm," *Sensors Actuators, A Phys.*, vol. 235, pp. 105–118, Nov. 2015. DOI: 10.1016/j.sna.2015.09.043.

[14] S. B. Choi, S. K. Lee, and Y. P. Park, "A hysteresis model for the field-dependent damping force of a magnetorheological damper," *Journal of Sound and Vibration*, vol. 245, no. 2. Academic Press, pp. 375–383, Aug. 2001. DOI: 10.1006/jsvi.2000.3539.

[15] X. Song, M. Ahmadian, and S. Southward, "Analysis and strategy for superharmonics with semiactive suspension control systems," *J. Dyn. Syst. Meas. Control. Trans. ASME*, vol. 129, no. 6, pp. 795–803, Nov. 2007. DOI: 10.1115/1.2789470.

[16] M. Yu, C. R. Liao, W. M. Chen, and S. L. Huang, "Study on MR Semi-active Suspension System and its Road Testing," *J. Intell. Mater. Syst. Struct.*, vol. 17, no. 8–9, pp. 801–806, Sep. 2006. DOI: 10.1177/1045389X06057534.

[17] Y. Shen, M. F. Golnaraghi, and G. R. Heppler, "Load-leveling suspension system with a magnetorheological damper," *Veh. Syst. Dyn.*, vol. 45, no. 4, pp. 297–312, Apr. 2007. DOI: 10.1080/00423110600928721.

[18] S. R. Hong *et al.*, "Analytical and experimental validation of a nondimensional Bingham model for mixed-mode magnetorheological dampers," *J. Sound Vib.*, vol. 312, no. 3, pp. 399–417, May 2008. DOI: 10.1016/j.jsv.2007.07.087.

[19] S. B. Choi, M. S. Seong, and S. H. Ha, "Vibration control of an MR vehicle suspension system considering both hysteretic behavior and parameter variation," *Smart Mater. Struct.*, vol. 18, no. 12, p. 125010, Sep. 2009. DOI: 10.1088/0964-1726/18/12/125010.

[20] S. Talatahari *et al.*, "Tribe–charged system search for parameter configuration of nonlinear systems with large search domains," *Eng. Optim.*, vol. 53, no. 1, pp. 18–31, Jan. 2021. DOI: 10.1080/0305215X.2019.1696786.

[21] M. Bozorgvar and S. M. Zahrai, "Semi-active seismic control of buildings using MR damper and adaptive neural-fuzzy intelligent controller optimized with genetic algorithm," *J. Vib. Control*, vol. 25, no. 2, pp. 273–285, Jan. 2019. DOI: 10.1177/1077546318774502.

[22] S. Gad *et al.*, "Multi-objective genetic algorithm fractional-order PID controller for semi-active magnetorheologically damped seat suspension," *J. Vib. Control*, vol. 23, no. 8, pp. 1248–1266, May 2017. DOI: 10.1177/1077546315591620.

[23] M. Mohebbi, H. Dadkhah, and H. Rasouli Dabbagh, "A genetic algorithm–based design approach for smart base isolation systems," *J. Intell. Mater. Syst. Struct.*, vol. 29, no. 7, pp. 1315–1332, Apr. 2018. DOI: 10.1177/1045389X17733058.

[24] Y. Chen, Y. Yao, and Y. Zhang, "A Robust State Estimation Method Based on SOCP for Integrated Electricity-Heat System," *IEEE Trans. Smart Grid*, vol. 12, no. 1, pp. 810–820, Jan. 2021.

[25] Y. Chen, J. Ma, P. Zhang, F. Liu, and S. Mei, "Robust State Estimator Based on Maximum Exponential Absolute Value," *IEEE Trans. Smart Grid*, vol. 8, no. 4, pp. 1537–1544, Jul. 2017.

[26] Y. Chen, F. Liu, S. Mei, and J. Ma, "A Robust WLAV State Estimation Using Optimal Transformations," *IEEE Trans. Power Syst.*, vol. 30, no. 4, pp. 2190–2191, Jul. 2015.

[27] F. Raeesi *et al.*, "An inverse TSK model of MR damper for vibration control of nonlinear structures using an improved grasshopper optimization algorithm," *Structures*, vol. 26, pp. 406–416, Aug. 2020. DOI: 10.1016/j.istruc.2020.04.026.

[28] X. Lin, S. Chen, and G. Huang, "A shuffled frog-leaping algorithm based mixed-sensitivity H∞ control of a seismically excited structural building using MR dampers," *J. Vib. Control*, vol. 24, no. 13, pp. 2832–2852, Jul. 2018. DOI: 10.1177/1077546317695462.

[29] X. Lin, S. Chen, and W. Lin, "Modified crow search algorithm–based fuzzy control of adjacent buildings connected by magnetorheological dampers considering soil–structure interaction," *J. Vib. Control*, vol. 27, no. 1–2, pp. 57–72, Jan. 2021. DOI: 10.1177/1077546320923438.

[30] M. R. Azraai, G. Priyandoko, A. R. Yusoff, and M. F. F. A. Rashid, "Parametric optimization of magneto-rheological fluid damper

[31] H. Metered *et al.*, "Vibration Control of MR-Damped Vehicle Suspension System Using PID Controller Tuned by Particle Swarm Optimization," *SAE Int. J. Passeng. Cars - Mech. Syst.*, vol. 8, no. 2, pp. 426–435, Jul. 2015. DOI: 10.4271/2015-01-0622.

[32] M. H. Abbasi and H. Moradi, "Optimum design of tuned mass damper via PSO algorithm for the passive control of forced oscillations in power transmission lines," *SN Appl. Sci.*, vol. 2, no. 5, pp. 1–15, May 2020.

[33] D. Dan, Y. Chen, and B. Xu, "A PSO Driven Intelligent Model Updating and Parameter Identification Scheme for Cable-Damper System," 2015.

[34] V. K. Pathak and A. K. Singh, "Optimization of morphological process parameters in contactless laser scanning system using modified particle swarm algorithm," *Meas. J. Int. Meas. Confed.*, vol. 109, pp. 27–35, Oct. 2017.

[35] V. K. Pathak and A. K. Singh, "Effective Form Error Assessment Using Improved Particle Swarm Optimization," *MAPAN*, vol. 32.

[36] V. K. Pathak and A. K. Singh, "Form Error Evaluation of Noncontact Scan Data Using Constriction Factor Particle Swarm Optimization," *J. Adv. Manuf. Syst.*, vol. 16, no. 3, pp. 205–226, Sep. 2017.

[37] R. Eberhart and J. Kennedy, "New optimizer using particle swarm theory," in *Proceedings of the International Symposium on Micro Machine and Human Science*, Nagoya, Japan, 1995, pp. 39–43.

[38] K. Luu *et al.*, "A parallel competitive Particle Swarm Optimization for non-linear first arrival traveltime tomography and uncertainty quantification," *Comput. Geosci.*, vol. 113, pp. 81–93, Apr. 2018. DOI: 10.1016/j.cageo.2018.01.016.

[39] K. A. M. Nor, A. G. A. Muthalif, and A. N. Wahid, "Optimization in active vibration control: Virtual experimentation using COMSOL multiphysics - MATLAB integration," in *Proceedings - International Conference on Intelligent Systems, Modelling and Simulation*, Langkawi, Malaysia, 2015, pp. 385–389.

[40] S. Malik *et al.*, "Parameter Estimation of a PID Controller using Particle Swarm Optimization Algorithm," *Int. J. Adv. Res. Comput. Commun. sys.*, vol. 3, no. 3, Mar. 2014.

[41] A. ALFI, "PSO with Adaptive Mutation and Inertia Weight and Its Application in Parameter Estimation of Dynamic Systems," *Acta Autom. Sin.*, vol. 37, no. 5, pp. 541–549, May 2011. DOI: 10.1016/s1874-1029(11)60205-x.

[42] Y. Huang *et al.*, "Parameter Estimation of Fractional-Order Chaotic Systems by Using Quantum Parallel Particle Swarm Optimization Algorithm," *PLoS One*, vol. 10, no. 1, p. e0114910, Jan. 2015. DOI: 10.1371/journal.pone.0114910.

[43] M. Clerc and J. Kennedy, "The particle swarm-explosion, stability, and convergence in a multidimensional complex space," *IEEE Trans. Evol. Comput.*, vol. 6, no. 1, pp. 58–73, Feb. 2002. DOI: 10.1109/4235.985692.

[44] LORD Corporation, "LORD TECHNICAL DATA: RD-8040-1 and RD-8041-1 Dampers," Cary, NC, Feb. 22, 2021. [Online]. Available: http://www.lordfulfillment.com/upload/DS7016.pdf

[45] B. F. Spencer *et al.*, "Phenomenological Model for Magnetorheological Dampers," *J. Eng. Mech.*, vol. 123, no. 3, pp. 230–238, Mar. 1997. DOI: 10.1061/(asce)0733-9399(1997)123:3(230).

Asan G. A. Muthalif (M'99, SM'16) received Bachelor and Masters in Mechatronics Engineering from International Islamic University Malaysia (IIUM), and a PhD degree from the Cambridge University, U.K., in 2008. He is currently an Associate Professor at the Dept. of Mechanical and Industrial Engineering,

This article has been accepted for publication in a future issue of this journal, but has not been fully edited. Content may change prior to final publication. Citation information: DOI 10.1109/ACCESS.2021.3080432, IEEE Access

Muthalif et al.: Preparation of Papers for IEEE Access (April 2021)

Qatar University. His research interests are on Mechatronics, Active & Semi-Active vibration control, Smart Materials and Structures, Vibration-based energy harvesting, Mid-High frequency vibration control, Statistical Energy Analysis (SEA), and Dynamics of built-up structures.

M. Khusyaie M. Razali received his Bachelor degree in Mechatronics Engineering from International Islamic University Malaysia (IIUM) in 2015. He obtained his Master's Degree in Mechatronics Engineering from IIUM in 2019. He worked as a Research Assistant in the Smart Structures, Systems and Control Research Lab in the Department of Mechatronic Engineering in IIUM. His research interests are in Mechatronics, Vibration Control, and Smart Materials.

N.H. Diyana Nordin obtained her PhD in Engineering from International Islamic University Malaysia (IIUM) in 2018. He is currently serving the university as an Assistant Professor at the Department of Mechatronics Engineering. Her research interests include semi-active vibration control, smart materials and applications, as well as biomechatronics.

Syamsul Bahrin Abdul Hamid received his Bachelor Degree in Electromechanical Power Engineer from Loughborough University in 1997, UK and Masters Degree in System Engineering with Information Technology from Cardiff University, UK, in 2006. He then received his PhD degree from the University of Strathclyde, UK, in 2014. He is currently an Assistant Professor at the Dept. of Mechatronics Engineering, International Islamic University Malaysia (IIUM). His research interests are in Mechatronics, Artificial Intelligence, Health Assistive Devices, Renewable Energy and Smart Infrastructure.